Final Report for AOARD Grant 114054
"**Nanoscale Investigation of New Fe-based Superconductors**"

Date: October 15, 2012

Name of Principal Investigators: Maw-Kuen Wu
- e-mail address: mkwu@phys.sinica.edu.tw; mkwu@mail.ndhu.edu.tw
- Institution : Institute of Physics, Academia Sinica
- Mailing Address : #128, Section 2, Academia Road, Nankang, Taipei, 11529 Taiwan
  Or (Current) : Office of the President, National Donghwa University
  Mailing Address: 1, Sec. 2, University Road, Shoufeng, Hualien, Taiwan
- Phone : +886-3-863-2001
- Fax : +886-3-863-2000

Period of Performance: 07/01/2011 – 12/31/2012

Abstract:

We have successfully synthesized high quality β-FeSe-type iron chalcogenide nanowires (NWs) from annealing thin films prepared by pulse laser deposition method. Three kinds of NWs with nominal composition (FeSe$_{0.9}$, FeSe$_{0.3}$Te$_{0.7}$ and FeTe$_{0.8}$S$_{0.2}$) have been prepared and carefully characterized by transmission electron microscope (TEM). Most analyzed NWs reveal good tetragonal structure along the (100) crystal direction. The energy dispersive spectroscopy studies and high resolution TEM (HRTEM) image demonstrate good compositional uniformity, except a thin layer of oxide on the surface. The FeSe$_{0.9}$ NWs don't show superconductivity because of highly Se rich. The other two types of NWs show a high and sharp superconducting transition. In addition, a transition tail is observed in the NWs with size smaller than 100nm, which might be due to the thermally activated phase slip effect.

Introduction:

Iron chalcogenides have received renewed attention following the unexpected discovery of superconductivity in tetragonal PbO-type β-FeSe with critical temperature (Tc) of 8K [1]. The superconducting transition temperature can be enhanced to 15K and 10K by substituting tellurium and sulphur respectively [2,3]. Recently, Xue *et al.* reported a zero resistance at 30K and an onset temperature over 55K in one unit cell FeSe film on SrTiO$_3$ substrate [4]. In addition, a clear diamagnetic signal around 40K was observed in as-grown FeSe nano-particles [5]. These results indicate that interesting phenomena may happen in iron chalcogenide superconductors when their size goes to nanometer scale.

Comparing with other two kinds of nano-scale samples, ultrathin film and

Report Documentation Page		*Form Approved* *OMB No. 0704-0188*

Public reporting burden for the collection of information is estimated to average 1 hour per response, including the time for reviewing instructions, searching existing data sources, gathering and maintaining the data needed, and completing and reviewing the collection of information. Send comments regarding this burden estimate or any other aspect of this collection of information, including suggestions for reducing this burden, to Washington Headquarters Services, Directorate for Information Operations and Reports, 1215 Jefferson Davis Highway, Suite 1204, Arlington VA 22202-4302. Respondents should be aware that notwithstanding any other provision of law, no person shall be subject to a penalty for failing to comply with a collection of information if it does not display a currently valid OMB control number.

1. REPORT DATE **23 OCT 2012**	2. REPORT TYPE **Final**	3. DATES COVERED **13-04-2011 to 12-10-2012**
4. TITLE AND SUBTITLE **Nanoscale Investigation of New Iron-Based Superconductors**		5a. CONTRACT NUMBER **FA23861114054**
		5b. GRANT NUMBER
		5c. PROGRAM ELEMENT NUMBER
6. AUTHOR(S) **Maw-Kuen Wu**		5d. PROJECT NUMBER
		5e. TASK NUMBER
		5f. WORK UNIT NUMBER
7. PERFORMING ORGANIZATION NAME(S) AND ADDRESS(ES) **Academia Sinica,128 Academia Rd., Section 2,Nankang, Taipei 11529,Taiwan,TW,11529**		8. PERFORMING ORGANIZATION REPORT NUMBER **N/A**
9. SPONSORING/MONITORING AGENCY NAME(S) AND ADDRESS(ES) **AOARD, UNIT 45002, APO, AP, 96338-5002**		10. SPONSOR/MONITOR'S ACRONYM(S) **AOARD**
		11. SPONSOR/MONITOR'S REPORT NUMBER(S) **AOARD-114054**

12. DISTRIBUTION/AVAILABILITY STATEMENT
Approved for public release; distribution unlimited

13. SUPPLEMENTARY NOTES

14. ABSTRACT
The researchers have successfully synthesized high quality β-FeSe-type iron chalcogenide nanowires (NWs) from annealing thin films prepared by pulse laser deposition method. Three kinds of NWs with nominal composition ($FeSe_{0.9}$, $FeSe_{0.3}Te_{0.7}$ and $FeTe_{0.8}S_{0.2}$) have been prepared and carefully characterized by transmission electron microscope (TEM). Most analyzed NWs reveal good tetragonal structure along the (100) crystal direction. The energy dispersive spectroscopy studies and high resolution TEM (HRTEM) image demonstrate good compositional uniformity, except a thin layer of oxide on the surface. The $FeSe_{0.9}$ NWs don?t show superconductivity because they are highly Se rich. The other two types of NWs show a high and sharp superconducting transition. In addition, a transition tail is observed in the NWs with size smaller than 100nm, which might be due to the thermally activated phase slip effect.

15. SUBJECT TERMS
Superconducting Materials, Nanocrystalline Materials, nanowires

16. SECURITY CLASSIFICATION OF:			17. LIMITATION OF ABSTRACT	18. NUMBER OF PAGES	19a. NAME OF RESPONSIBLE PERSON
a. REPORT **unclassified**	b. ABSTRACT **unclassified**	c. THIS PAGE **unclassified**	**Same as Report (SAR)**	**12**	

Standard Form 298 (Rev. 8-98)
Prescribed by ANSI Std Z39-18

nano-particles, crystalline nanowire (NW) in general is more difficult to be prepared. NWs can be artificially made through thin film deposition and nano-patterning technologies. Nevertheless, naturally grown crystalline NW is expected to be superior to the artificially made NWs in many aspects, which can be used for fundamental property studies. For example, several reports have demonstrated better superconducting properties in crystalline NWs [6, 7]. Crystalline superconducting NWs are commonly used to study superconductivity related phenomena, such as superconducting phase slip [8-11], anti-proximity effect [12], interplay between superconductivity and ferromagnetism [13], and quantum oscillation [14].

Growths of non-superconducting crystalline iron chalcogenide NWs have been reported, such as FeS_2 grown by solvothermal process [15] and thermal sulfidation [16], and Fe_7S_8 grown by electrodeposition method on anodic aluminum oxide (AAO) templates [17]. However, there was no report of the PbO-type iron chalcogenide NWs yet so far. This report describes the first time the growth and characterization of PbO-type iron chalcogenide superconducting NWs with nominal composition of $FeSe_{0.9}$, $FeSe_{0.3}Te_{0.7}$ and $FeTe_{0.8}S_{0.2}$.
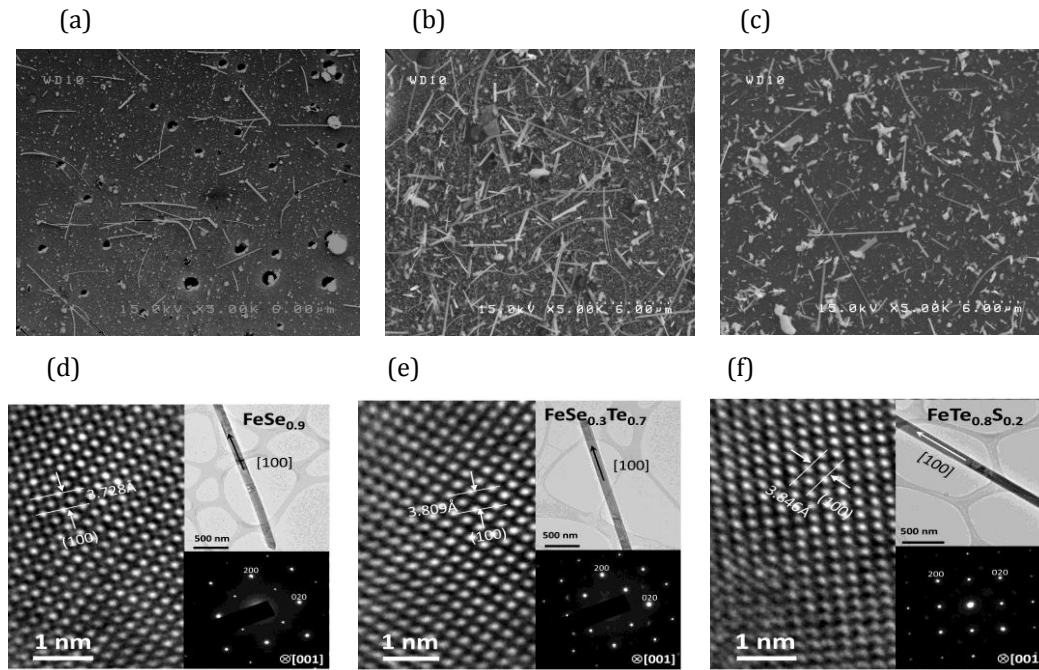

Figure 1 (a)-(c) SEM images of as-grown NWs on substrate. The nominal composition of thin film is (a) $FeSe_{0.9}$, and (b), $FeSe_{0.3}Te_{0.7}$, and (c) $FeTe_{0.8}S_{0.2}$. NWs are tens to hundreds nanometer in diameter and several to tens micrometer in length. (d)-(f) The HRTEM images and diffraction pattern of NWs. The NWs are grown along [100] direction. The a-axis lattice constant is 3.728Å, 3.809 Å, and 3.846 Å for $FeSe_{0.9}$, $FeSe_{0.3}Te_{0.7}$, and $FeTe_{0.8}S_{0.2}$ NWs respectively.

Growth and Structure Characterization of Nanowires

The synthesis of PbO-type iron chalcogenide NWs follows a simple

two-step process; so call on-film formation of NWs (OFF-ON) method [18]. First, th PbO-type iron chalcogenide thin films on (100) MgO substrate are prepared by pulse laser deposition (PLD) technique [19]. Then these films are sealed in vacuumed quartz tube and annealed at 400℃ for 120 hours for NW growth. NWs with nominal composition of $FeSe_{0.9}$, $FeSe_{0.3}Te_{0.7}$, and $FeTe_{0.8}S_{0.2}$ were prepared. NWs prefer to grow near the edge of thin film. The as-grown NWs are easily detached from substrate for property characterization.

Figure 1 (a)-(c) show the SEM images of as-grown PbO-type iron chalcogenide NWs on substrate. The NWs are tens to hundreds nanometers in diameter and several to tens micrometers in length. In general, number density and size of $FeSe_{0.9}$ NWs are lower and smaller. The high resolution transmission electron microscope (HRTEM) images demonstrate excellent crystalline of tetragonal structure in these NWs, as shown in Fig. 1 (d)-(f). The growth of NWs is found to be along [100] direction, as indicated in the sets. The X-ray diffraction patterns demonstrate good square lattice in ab-plane.
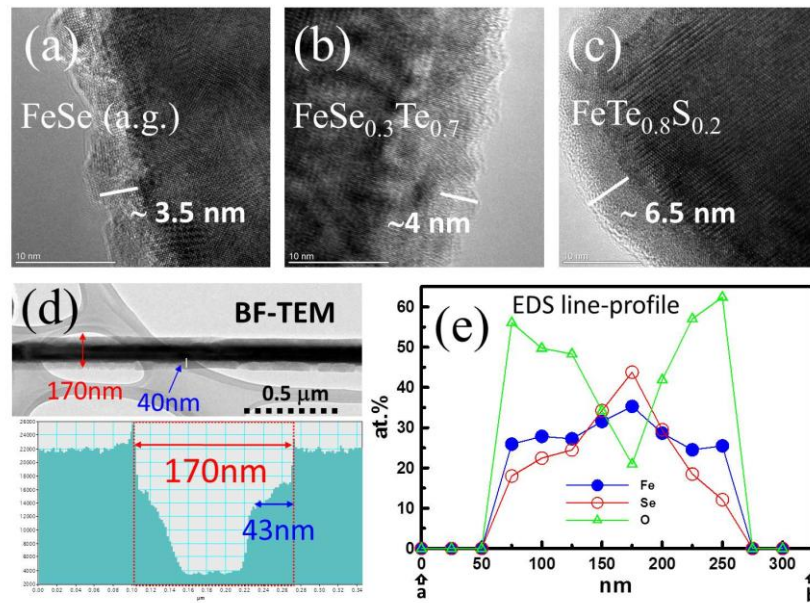

Figure 2 Surface oxidation of NWs. (a)-(c) The HRTEM images show an oxide layer of few nanometers on the surface of as-grown NWs. (d) BF-STM image and line profile illustrate an oxide layer of 40nm thickness on the surface of 170nm $FeSe_{0.9}$ NW six months later. (e) The EDS line profiles of iron, selenium, and oxygen. Oxygen becomes dominant except of the center of NW, verifying the existence of thick oxide layer on the surface.

It has been reported that the surface of PbO-type iron chalcogenide can be easily oxidized [20, 21]. It is important to know the thickness and growth rate of oxide layer after NWs are grown because this oxide layer needs to be removed before metal deposition for electrical contact. The HRTEM image of NW shows an

amorphous layer at edge, which is identified as the surface oxide. The as-grown NW has a few nanometers thick oxide layer on the surface, as illustrated in Figure 2 (a)-(c). After stored in a vacuumed desiccator for two months, the oxide layer becomes about 10nm thick, not shown in this paper. The growth rate of surface oxide is similar for $FeSe_{0.9}$, $FeSe_{0.3}Te_{0.7}$, and $FeTe_{0.8}S_{0.2}$ NWs. Figure 2(d) shows the back field TEM image and EDS line profile of a 170nm $FeSe_{0.9}$ NW six months after growth. The amorphous layer increases to 40nm thick, which is about 5-10 times thicker. The EDS line-profile demonstrates high oxygen and iron concentration except of center area, as shown in Fig. 2(e), indicating that this amorphous layer is iron oxide.
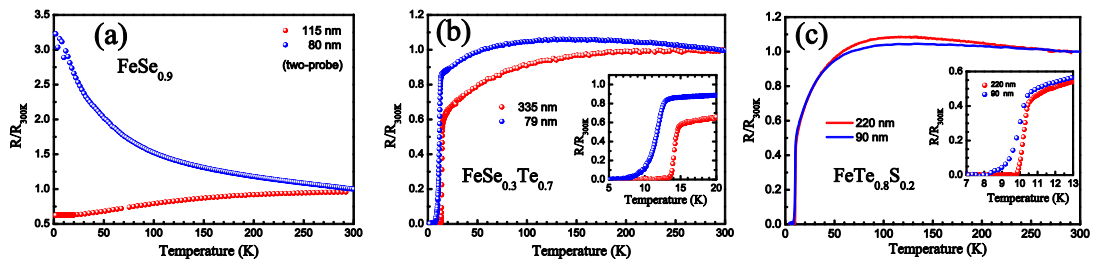

Figure 3 The normalized resistance of NWs with different size. (a) $FeSe_{0.9}$ NWs with size of 115nm and 80nm. (b) $FeSe_{0.3}Te_{0.7}$ NWs with size of 335nm and 79nm. (c) $FeTe_{0.8}S_{0.2}$ NWs with size of 220nm and 90nm. A long transition tail is observed in both $FeSe_{0.3}Te_{0.7}$ and $FeTe_{0.8}S_{0.2}$ NWs with small size.

Superconductivity of nanowires

Most $FeSe_{0.9}$ NWs show insulating or high resistance. Figure 3(a) present the normalized resistance versus temperature curves of $FeSe_{0.9}$ NWs which have lower resistance. No superconducting transition is observed in both NWs. To investigate the reason responsible for vanish of its superconductivity, we analyze the chemical composition of many NWs by energy dispersive X-ray spectroscopy (EDS). All NWs have good uniformity in composition but chalcogen rich. The average ration of Se/Fe is about 1.26, which is too high to be ⬚-FeSe phase [22]. However, the results of HRTEM and X-ray diffraction demonstrate a good tetragonal crystal structure with lattice constants of a=3.728Å and c=5.363 Å, which are much smaller than that of ⬚-$FeSe_x$ bulk sample (a=3.775Å and c=5.512 Å) [23]. Based on these results, our $FeSe_{0.9}$ NWs might be ⬚'-FeSe phase which structure is tetragonal with wider Se concentration range, 48.5~62 at% or 0.94~1.63 in Se/Fe ratio and smaller lattice constant in Se rich sample [22]. Recently, M. de Souza et. al. reported a superconducting transition at 8.5K in ⬚'-$Fe_{0.91}Se$ (or ⬚'-$FeSe_{1.1}$) sample which synthesized under high pressure [24]. However, the Se concentration in our $FeSe_{0.9}$ NWs is still too high, resulting in insulating or high resistive characteristic. We believe that b-FeSe phase NWs could be prepared by using a Se-deficient thin film or reducing the annealing
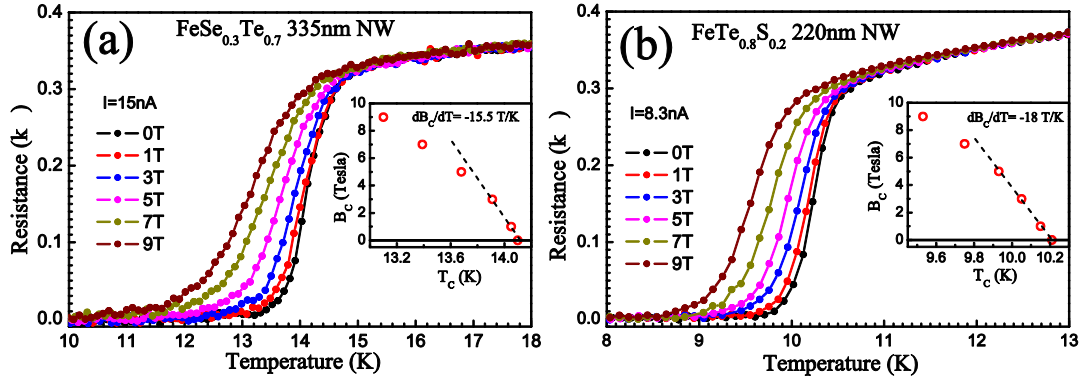
temperature.

Figure 4 Magnetic field dependence of superconducting transition of (a) $FeSe_{0.3}Te_{0.7}$ and (b) $FeTe_{0.8}S_{0.2}$ NWs. The phase diagram is shown in the insets. The upper critical field is estimated to be 151 and 127 Tesla for $FeSe_{0.3}Te_{0.7}$ and $FeTe_{0.8}S_{0.2}$ NW respectively, using the WHH formula [32] and the initial slope of phase diagram in the inset.

On the contrary, sharp superconducting transition at 14.5 K and 10.3 K is observed in $FeSe_{0.3}Te_{0.7}$ and $FeTe_{0.8}S_{0.2}$ NWs with a size of 335nm and 220nm respectively, as shown in Fig. 4(b) and 4(c). The EDS data shows that the ratio of Se/Te and S/Te is 0.33/0.67 and 0.08/0.92. Comparing with bulk/film/crystal samples with similar composition [2, 25-27], these NWs have slightly higher transition temperature and much narrower transition width. Beside of superconducting properties, most reports on high Te substituted $FeSe_{1-x}Te_{x}$ samples have semiconducting-like temperature dependence at low temperature. Chang *et. al.* reported that such temperature dependence is attributed to weak localization effect which results from high scattering rate of carriers by impurities [28]. The NWs have metallic-like temperature dependence, indicating a lower impurity concentration or better crystalline quality. For NWs with smaller size, also shown in in Fig. 4(b) and 4(c), the superconducting temperature is slightly lower, but with a long transition tail. We rule out the possibility of quality degradation in small size NW because their TEM results demonstrate similar crystal quality. Because of the existence of surface oxide, the dimension of actual superconducting area is smaller than the outer dimension of NWs. Moreover, we expect a thicker oxide layer in those NWs after exposed to air and fabricating process for making electrical leads, such as shown in Fig. 2(d). The dimension of superconducting area should be much reduced and the thermally activated phase slip (TAPS) effect might become important [29, 30], resulting in a long transition tail.

Figure 4 shows the magnetic field dependence of superconducting transition of (a) $FeSe_{0.3}Te_{0.7}$ and (b) $FeTe_{0.8}S_{0.2}$ NWs. The superconducting transition tail is slightly broadened in $FeSe_{0.3}Te_{0.7}$ NW as external magnetic field

applied, which is similar to results of bulk [31] and crystal [25]. For FeTe$_{0.8}$S$_{0.2}$ NW, superconducting transition shifts almost in parallel to low temperature, which is same as the earlier reports [3, 27]. The insets demonstrate the phase diagram of NWs. According to WHH theory [32], the critical magnetic field at zero temperature can be estimated from the initial slope of phase diagram, $H_{c2}(0) = 0.693|dH_{c2}/dt|$, where t is the reduced temperature, $T_C(H)/T_C(0)$. The estimated $H_{C2}(0)$ of 335nm FeSe$_{0.3}$Te$_{0.7}$ and 220nm FeTe$_{0.8}$S$_{0.2}$ NWs is 151 and 127 Tesla, respectively. These values are higher than the reported values, ~100 Tesla for FeSe$_{0.3}$Te$_{0.7}$ [31] and 70 Tesla for FeTe$_{0.8}$S$_{0.2}$ [3] bulk samples.

Conclusions

High quality NWs are helpful in studying the intrinsic properties of newly discovered iron chalcogenide superconductors. In this paper, we have presented a simple two-step method to synthesize highly crystalline iron chalcogenide NWs. Three kinds of NWs with nominal composition (FeSe$_{0.9}$, FeSe$_{0.3}$Te$_{0.7}$ and FeTe$_{0.8}$S$_{0.2}$) have been prepared and carefully characterized by TEM. The NWs show highly crystalline along the (100) crystal direction. A few nanometers thick oxide is observed on the surface in fresh NWs, and becomes thicker gradually as exposed to air. The FeSe$_{0.9}$ NWs demonstrate tetragonal structure with smaller lattice constant, highly Se rich, and high resistance. We speculate that the grown FeSe$_{0.9}$ NWs might be ⍰'-FeSe phase, rather than ⍰-FeSe phase. Comparing with bulk samples, FeSe$_{0.3}$Fe$_{0.7}$ and FeTe$_{0.8}$S$_{0.2}$ NWs reveal a high and sharp superconducting transition. Combining with the results of normal state resistance behavior and upper magnetic critical field, we conclude that these FeSe$_{0.3}$Fe$_{0.7}$ and FeTe$_{0.8}$S$_{0.2}$ NWs have excellent quality. More intrinsic properties of iron chalcogenide superconductors can be studied by using these NWs. In addition, the FeSe$_{0.3}$Fe$_{0.7}$ and FeTe$_{0.8}$S$_{0.2}$ NWs with size smaller than 100nm always show a long resistive transition tail. We ruled out the possibility of non-uniformity either in stoichiometry or in size. The most possible reason responsible for this phenomenon is the thermally activated phase slip effect. More detail experiment will be done to verify our speculation.

Acknowledgement

Reference:

[1] F.C. Hsu, J.Y. Luo, K.W. Yeh, T.K. Chen, T.W. Huang, Wu, Phillip M., Y.C. Lee, Y.L. Huang, Y.Y. Chu, D.C. Yan, M.K. Wu, *Proceedings of the National Academy of Sciences*, **105**, 14262 (2008)

[2] K. W. Yeh, T. W. Huang, Y. L. Huang, T. K. Chen, F. C. Hsu, P. M. Wu,Y. C. Lee, Y. Y. Chu, C. L. Chen, J. Y. Luo, D. C.g Yan, and M. K. Wu, *EPL (Europhysics Letters)* **84** 37002 (2008)

[3] Y. Mizuguchi, F. Tomioka, S. Tsuda, T. Yamaguchi, and Y. Takano, *Appl. Phys. Lett.* **94**, 012503 (2009)

[4] Q.Y. Wang, Z. Li, W. H. Zhang, Z. C. Zhang, J. S. Zhang, W. Li, H. Ding, Y. B. Ou, P. Deng, K. Chang, J. Wen, C. L. Song, K. He, J. F. Jia, S. H. Ji, Y. Y. Wang, L. L. Wang, X. Chen, X. C. Ma, Q. K. Xue, *Chin. Phys. Lett.* **29**(3) 037402 (2012).[5] Unpublished data.

[6] G. Yi and W. Schwarzacher, *Appl. Phys. Lett.* **74**(12), 1746-1748 (1999)

[7] A. K Jha and N. Khare, *Supercond. Sci. Technol.* **22,** 075017(2009)

[8] J. G. Wang, M. L. Tian, N. Kumar, and T. E. Mallouk, *Nano Letters*, **5**(7). 1247-1253 (2005)

[9] M. L. Tian, J. G. Wang, J. S. Kurtz, Y. Liu, M. H. W. Chan, T. S. Mayer, and T. E. Mallouk, *Phys. Rev. B* **71**, 104521 (2005)

[10] K. Y. Arutyunov, D. S. Golubev, and A. D. Zaikin, *Phys. Rep.* **464**, 1 (2008).

[11] J. Wang, Y. Sun, M. L. Tian, B. Z. Liu, M. Singh, and M. H. W. Chan, *Phys. Rev. B* **86**, 035439 (2012)

[12] M. Singh, J. Wang, M. L. Tian, T. E. Mallouk, and M. H. W. Chan, *Phys. Rev. B* **83**, 220506(R) (2011)

[13] J. Wang, M. Singh, M. L. Tian, N. Kumar, B. Z. Liu, C. T. Shi, J. K. Jain, N. Samarth, T. E. Mallouk, and M. H.W. Chan, *Nature Physics*, 6, 389-394 (2010)

[14] M. L. Tian, J. Wang, Q. Zhang, N. Kumar, T. E. Mallouk, and M. H. W. Chan, *Nano Letters*, **9**(9), 3196-3202 (2009)

[15] S. Kar and S. Chaudhuri, *Chem. Phys. Lett.* **398** 22-26 (2004)

[16] M. Cabán-Acevedo, M. S. Faber, Y. Z. Tan, R. J. Hamers, and S. Jin, *Nano Lett.* **12**, 1977–1982 (2012)

[17] G. H. Yue, P. X. Yan, X. Y. Fan, M. X. Wang, D. M. Qu, D. Yan, and J. Z. Liu, *J. Appl. Phys.* **100** 124313 (2006)

[18] W. Y. Shim, J. H. Ham, K. I. Lee, W. Y. Jeung, M. Johnson, and W. Y. Lee, *Nano letters* **9** 18-22 (2009)

[19] M. K. Wu, F.C. Hsu, K.W. Yeh, T.W. Huang, J.Y. Luo, M. J.Wang, H. H. Chang, T. K. Chen, S. M. Rao, and B. H. Mok et al., *Physica C* **469**, 340 (2009).

[20] C. L. Chen, S. M. Rao, C. L. Dong, J. L. Chen, T. W. Huang, B. H. Mok, M. C. Ling,

W. C. Wang, C. L. Chang, T. S. Chan, J. F. Lee, J.-H. Guo and M. K. Wu, *EPL*, **93**, 47003 (2011)

[21] C. L. Chen, C. L. Dong, J. L. Chen, J.-H. Guo, W. L. Yang, C. C. Hsu, K. W. Yeh, T. W. Huang, B. H. Mok, T. S. Chan, J. F. Lee, C. L. Chang, S. M. Rao and M. K. Wu, *Phys. Chem. Chem. Phys.*, **13**, 15666–15672 (2011)

[22] H. Okamoto, *J. Phase Equilibria* 12(3) 384 (1991)

[23] Z. F. Li, J. Ju, J. Tang, K. Sato, M. Watahiki, K. Tanigaki, *J. Phys. Chem. Solids* **71,** 495(2010)

[🗆🗆] M. de Souza, A.-A. Haghighirad, U. Tutsch, W. Assmus, and M. Lang, *Eur. Phys. J.* B **77**, 101–107 (2010)

[25] K. W. Yeh, C. T. Ke, T. W. Huang, T. K. Chen, Y. L. Huang, P. M. Wu, and M. K. Wu, *Crystal Growth & Design*, **9**(11), 4847–4851 (2009)

[26] Y. Mizuguchi, F. Tomioka, S. Tsuda, T. Yamaguchi, and Y. Takano, *J. Phys. Soc. Jpn.* **78,** 074712 (2009)

[27] Y. Mizuguchi1, K. Deguchi, S. Tsuda, T. Yamaguchi, and Y. Takano, *EPL* **90** 57002 (2010)

[28] H. H. Chang, J. Y. Luo, C. T. Wu, F. C. Hsu, T. W. Huang, P M Wu, M. K. Wu, and M. J. Wang, *Supercond. Sci. Technol.*, **25,** 035004 (2012)

[29] J. S. Langer, V. Ambegaokar, *Phys. Rev.* **164**, 498 (1967)

[30] D. E. McCumber, B. I. Halperin, *Phys. Rev. B*, **1**, 1054 (1970)

[31] K.W. Yeh, H.C. Hsu, T.W. Huang, P.M. Wu, Y.L. Huang, T.K. Chen, J.Y. Luo, and M.K. Wu, *J. Phys. Soc. Jpn.* **77**, *Suppl. C*, pp. 19-22 (2008)

[32] N. R. Werthamer,E. Helfand, and P. C. Hohenberg, *Phys. Rev.* **147**, 295 (1966).

List of Publications (partially supported by this grant):

"The vortex state of FeSe(1-x)Te(x) superconducting thin films", Chang HH, Luo JY , Wu CT, FC Hsu, TW Huang, PM Wu, MK Wu, MJ Wang, SUPERCONDUCTOR SCIENCE & TECHNOLOGY, 24, 105011, (2011).

"Convective solution transport -An improved technique for the growth of big crystals of the superconducting alpha-FeSe using KCl as solvent", SM Rao, BH Mok, MC Ling ,CT Ke, TC Chen, IM Tsai, YL Lin, HL Liu,CL Chen, FC Hsu, TW Huang, TB Wu, MK Wu, JOURNAL OF APPLIED PHYSICS, 110, 113919, (2011).

"Superconductivity in PbO-type tetragonal FeSe nanoparticles", Chang, CC ; Wang, CH; Wen, MH; Wu, YR; Hsieh, YT ; Wu, MK, SOLID STATE COMMUNICATIONS, 152, 649-652 (2012).

"Weak localization in FeSe1-xTex superconducting thin films", Chang, HH, Luo, JY, Wu, CT, Hsu, FC, Huang, TW, Wu, PM, Wu, MK, Wang, MJ, SUPERCONDUCTOR SCIENCE & TECHNOLOGY, 25, 035004 (2012).

"Convective solution transport-An improved technique for the growth of big crystals of the superconducting alpha-FeSe using KCl as solvent", Rao, S. M., Mok, B. H., Ling, M. C., Ke, C. T., Chen, T. K., Tsai, I. -M., Lin, Y.-L., Liu, H. L., Chen, C. L., Hsu, F. C., Huang, T. W., Wu, T. B., Wu, M. K., JOURNAL OF APPLIED PHYSICS, April, (2012).

"Gap opening and orbital modification of superconducting FeSe above the structural distortion", Y.-C. Wen, K.-J. Wang, H.-H. Chang, J.-Y. Luo, C.-C. Shen, H.-L. Liu, C.-K. Sun, M.-J. Wang, and M.-K. Wu, Phys. Rev. Letts., 108, 275002, (2012).

Experiment: Description of the experiment performed and the facilities used to perform the work.

Results and Discussion: Describe the results obtained during the period of performance and what work may be performed in the future as follow on.

List of Publications: Please list any publications, conference presentations, or patents that resulted from this work.

DD882: As a separate document, please complete and sign the inventions disclosure form.

This document may be as long or as short as needed to give a fair account of the work performed during the period of performance. There will be variations depending on the scope of the work. As such, there is no length or formatting constraints for the final report. Include as many charts and figures as required to explain the work. A final report submission very similar to a full length journal article will be sufficient in most cases.